Weak localization in lateral surface superlattices

M. Suhrke
Institut für Theoretische Physik, Universität Regensburg, Universitätsstraße 31, D-93053 Regensburg, Germany

P. E. Selbmann
Max-Planck-Arbeitsgruppe Halbleitertheorie, Hausvogteiplatz 5-7, D-10117 Berlin, Germany
(Received 18 June 1993; revised manuscript received 18 August 1993)

We present a theoretical investigation of weak localization in a two-dimensional electron gas with unidirectional modulation by a cosine potential. By lowering the electron density the system gradually turns from a weakly modulated electron gas into an array of almost isolated quantum wires of finite width. A dimensional transition occurs in such a system due to the decreasing widths of the resulting minibands. The reduction of the dimensionality of interference effects takes place when coherent tunneling of electrons between adjacent wires is suppressed. In this case we find a pronounced enhancement of the weak-localization correction to the conductivity. Its functional dependence on the phase coherence length develops from a logarithmic behavior to a linear one, typical for one dimension. Close to the transition to strong localization the correction due to interference effects becomes additive in the resistance. The localization length deduced from the calculations exhibits a continuous change from an exponential to a linear dependence on the scattering length at the dimensional transition. Numerical results are discussed for GaAs structures with different electron densities.

I. INTRODUCTION

A two-dimensional electron gas (2DEG) laterally modulated by a periodic potential exhibits unusual features in transport experiments. A prominent example is an additional oscillatory behavior of the magnetoresistance at weak fields if the potential amplitude is small compared to the Fermi energy.[1,2] These oscillations are now well explained by theory.[3,4] Another interesting topic is carrier transport in strongly modulated structures representing an array of quantum wires for Fermi energies well below the potential amplitude.[5–9] Recently, the fabrication of an atomically precise one-dimensional (1D) superlattice within a 2DEG has been reported.[10]

There exists a number of theoretical calculations on the consequences of the electronic spectrum of lateral surface superlattices on transport properties (see, e.g., Refs. 11 and 12). The behavior of interference effects such as weak localization has been investigated less for these systems. Kearney and Butcher[13] have analyzed the 2D-1D transition of weak localization in a single quantum wire with many occupied subbands. This transition takes place if the phase coherence length is comparable to the wire width. Because their approach relies on the diffusion approximation this implies that the elastic scattering length has to be much smaller than the wire width. In that case one expects that no subband effects will be resolved. The influence of subband effects on weak localization and the transition to strong localization in a quantum wire has been studied in Refs. 14 and 15. Localization in anisotropic systems has been discussed for the case of anisotropic effective masses[16] and mainly in the context of coupled metallic wires.[17–19] The latter authors consider a one-band model in the tight binding approximation for the case of an open Fermi surface (Fermi energy much larger than band width) and analyze the Anderson transition as well as the dependence of weak localization on a perpendicular magnetic field which tunes the dimensionality of the system. Szott *et al.*[20] have applied a similar model to a system of coupled strictly 1D strips in order to investigate weak localization in lateral surface superlattices. This means that in their calculation only one subband exists in a quantum wire which is very difficult to realize in experiments.

The aim of the present paper is to investigate the 2D-1D transition in weak localization in lateral surface superlattices with a periodic potential which models the experimental conditions sufficiently well. Typically, more than one one-dimensional subband will be occupied by charge carriers and their individual Fermi surfaces will be either closed or open depending on the position of Fermi energy in difference to the model analyzed in Refs. 17–19. In contrast to Ref. 13 we are interested in a situation where the total scattering length is much larger than the potential period. This means that it is much larger than the wire width in the 1D limit and, consequently, the electrons move ballistically across a single wire. Under these conditions the phase coherence length is much larger than the potential period, too, and one expects a transition from 2D to 1D behavior of weak localization if the Fermi energy is reduced below the potential amplitude. Due to the coupling of the different wires via tunneling there exists another mechanism of the 1D-2D transition of weak localization in our case compared to a single wire. When the phase coherence time of the electrons becomes larger than the tunneling time they can move coherently in *two* directions and the dimensional crossover is expected to take place. In the 1D limit of

isolated wires the system is expected to undergo a rapid transition to strong localization with increasing phase coherence length. This will be incorporated into our calculations via a self-consistent treatment of the interference effects and allows us to estimate the localization length in dependence on Fermi energy. The results will be seen to be similar to those for metallic wires[17–19] in the limiting case investigated by these authors.

II. MODEL OF THE SYSTEM

A. Structure

We describe the unidirectional modulation of the 2DEG located in the x-y plane by a cosine potential

$$V(y) = V_0 \cos(2\pi y/a) \tag{2.1}$$

of amplitude V_0 and period a which is applied in the y direction. The system is a weakly modulated 2DEG if the Fermi energy E_F is much larger than the amplitude V_0. It develops continuously to an array of almost decoupled quantum wires if the Fermi energy becomes smaller than the potential amplitude.

The solution of Schrödinger's equation in effective mass approximation yields plane waves in the x direction and Bloch functions in the y direction

$$\psi_{n\mathbf{k}}(\mathbf{r}) = A^{-1/2}\, e^{i\mathbf{k}\cdot\mathbf{r}}\, u_{nk_y}(y) \tag{2.2}$$

with the Bloch factors $u_{nk_y}(y)$. Here $\mathbf{r} = (x, y)$, $\mathbf{k} = (k_x, k_y)$ is the two-dimensional wave vector restricted to the first Brillouin zone $(-\pi/a, \pi/a)$ in the y direction, n is the band index, and A is the normalization area. The corresponding one-particle spectrum is given by

$$E_{n\mathbf{k}} = \frac{\hbar^2 k_x^2}{2m^*} + \varepsilon_{nk_y}\,, \tag{2.3}$$

where the ε_{nk_y} follow from the solution of Mathieu's equation[21] and m^* is the effective mass of the system without modulation. The spectrum ε_{nk_y} is shown in Fig. 1 for a modulation potential of amplitude $V_0 = 5$ meV and period of $a = 200$ nm which correspond to usual experimental values.[5–9]

B. Scattering model

Investigating weak localization one has to distinguish between elastic and inelastic scattering mechanisms, respectively. Elastic scattering leads to localization due to interference of electron waves. For the correlation function of the potential $U(\mathbf{r})$ of randomly distributed scattering centers we use the model of Gaussian white noise

$$\langle U(\mathbf{r})U(\mathbf{r}')\rangle = g^{\mathrm{el}}\delta(\mathbf{r}-\mathbf{r}')\,. \tag{2.4}$$

The symbol $\langle\,\rangle$ denotes the configurational average and g^{el} is the elastic coupling constant. This model, which is commonly used to describe disorder scattering, corresponds to short-ranged scatterers in real space, i.e., isotropic scattering in momentum space.

Inelastic scattering, which destroys interference effects by limiting the phase coherence of electron waves, is assumed here for simplicity to be short ranged, too. An example is scattering by acoustic phonons via deformation potential coupling in the usual approximations. Since both scattering mechanisms have the same energy dependence, the total coupling constant

$$g = g^{\mathrm{el}} + g^{\mathrm{in}} = e\hbar^3/m^{*2}\mu_{2\mathrm{D}} \tag{2.5}$$

is the sum of the elastic and inelastic ones and is given by the mobility $\mu_{2\mathrm{D}}$ of the 2DEG. The inelastic coupling constant can be related to the phase coherence length L_Φ via[15]

$$\Delta_\Phi \equiv g^{\mathrm{in}}/g = \Gamma_{\mathrm{in}}/\Gamma \equiv l_x^2/L_\Phi^2\,. \tag{2.6}$$

Here Γ_{in} and Γ are the inelastic and total scattering rates, respectively, and l_x is the total scattering length in the x direction. The latter becomes $l_x = l_{1\mathrm{D}}$ $(l_y \to 0)$ in the 1D limit of isolated quantum wires and $l_x = l_y = l_{2\mathrm{D}}/\sqrt{2}$ in the limit of the unmodulated 2DEG. The phase coherence length defined by Eq. (2.6) fulfills the correct relation $L_\Phi = \sqrt{\hbar D/\Gamma_{\mathrm{in}}}$ in these cases with the d-dimensional diffusion coefficient D.

The equilibrium properties of the system are determined by the one-particle Green function. For weak enough scattering ($E_F \gg \Gamma$) we can neglect interference effects in the one-particle properties and restrict ourselves to the self-consistent Born approximation. The self-energy is averaged over the period a of the modulation potential which makes it independent of the quan-

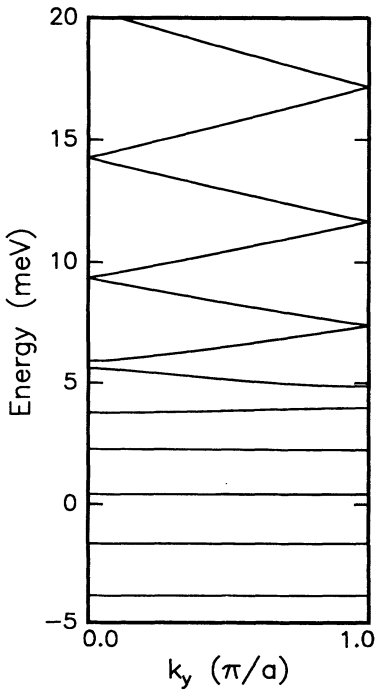

FIG. 1. Spectrum ε_{nk_y} for a modulation potential of amplitude $V_0 = 5$ meV and period $a = 200$ nm.

tum numbers n and $\mathbf{k}$ for short-range scattering.[22] Furthermore, we omit the real part of the self-energy which leads only to a shift of the energy zero. The resulting self-consistent equations for the imaginary part of the self-energy Γ are

$$\Gamma(E) = \pi g \varrho(E) = g \sum_{n\mathbf{k}} A_{n\mathbf{k}}(E) \ , \tag{2.7a}$$

$$A_{n\mathbf{k}}(E) = 2\,\mathrm{Im}\,[E - E_{n\mathbf{k}} - i\Gamma(E)/2]^{-1} \ , \tag{2.7b}$$

where $A_{n\mathbf{k}}(E)$ is the spectral function, i.e., the imaginary part of the one-particle Green function and $\varrho(E)$ is the density of states.

Numerical results for the density of states in dependence on energy are shown in Fig. 2 for the parameters of Fig. 1 and for two different scattering strengths. Here and in the following figures the arrow indicates the maximum of the modulation potential at 5 meV. For energies well below the maximum, $\varrho(E)$ behaves essentially as in one dimension. In that case one recognizes inverse-square-root-like singularities at the subband bottoms if scattering is weak enough. For stronger scattering they are broadened by lifetime effects included here in self-consistent Born approximation. The lowest subbands have approximately equal spacing in energy as expected if the cosine potential can be approximated by a parabolic one. Above the potential maximum the density of states approaches quickly its two-dimensional value which is energy independent. Just at the threshold the spectrum already shows dispersion in the y direction, but the bands are still well separated by gaps. This leads to a step-like onset of the density of states at the lower band edge and a logarithmic divergency at the upper band edge for negligible scattering as usual for a band of finite width in two dimensions. The energy dependence of the scattering rate is identical to that of the density of states because both differ only by a constant factor.

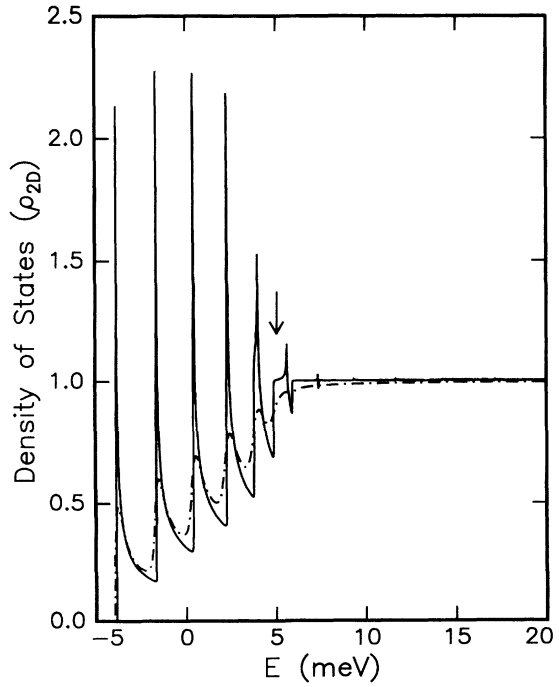

FIG. 2. Density of states in units of its value ϱ_{2D} of a two-dimensional system in dependence on energy for the parameters of Fig. 1. Two different scattering strengths are shown corresponding to mobilities of the 2D reference system $\mu_{2D} = 5 \times 10^6$ cm^2/V s (solid line) and $\mu_{2D} = 5 \times 10^4$ cm^2/V s (dashed line).

III. CONDUCTIVITY

In this section we turn to the calculation of transport properties of the system under consideration which are determined by the two-particle Green function. In contrast to the equilibrium properties, interference of electron waves is now no longer negligible, leading to weak localization even for $E_F \gg \Gamma$.[23,24] In terms of Green function perturbation theory this means that in addition to diagrams with noncrossed interaction lines corresponding to the self-consistent Born approximation, those with maximally crossed impurity lines (cooperon) have to be taken into account. We have done this by use of the nonequilibrium Green function technique. The principles of the calculation have been published elsewhere.[15] Note that it is convenient to perform the calculations in a real space representation (compare also Ref. 25) and to change then to a representation in the basis of the wave functions of the modulated system without scattering.

A. Self-consistent Born approximation

As a first step, we evaluate the conductivity of the system in self-consistent Born approximation. Without magnetic field and at zero temperature the diagonal tensor of band conductivities is given by

$$\sigma_{ii}^{B}(E_F) = \frac{e^2}{h} \sum_{n\mathbf{k}} \hbar^2 v_i^2 A_{n\mathbf{k}}^2(E_F), \quad v_i = \frac{\partial E_{n\mathbf{k}}}{\partial \hbar k_i} \tag{3.1}$$

with the group velocity v_i and $i = x, y$. Here we have omitted the nondiagonal elements of the velocity matrix element in the y direction which correspond to scattering-induced intersubband transitions. They are small in the parameter $\Gamma/\Delta E$ in the 1D limit where ΔE is the subband spacing and in the parameter V_0/E_F in the 2D limit. The result for finite temperature can be obtained from Eq. (3.1) by simply convolving it with the derivative of the Fermi function. It is obvious that the anisotropy of the system enters via the differing group velocities if the modulation potential becomes important. In particular, the group velocity in the y direction vanishes in the 1D limit if the spectrum shows no dispersion in this direction. The components of the conductivity tensor are shown in Fig. 3 for two different scattering strengths. The oscillations of decreasing amplitude for energies below the potential maximum arise from the population of 1D subbands. With increasing scattering strength they become broadened by lifetime effects. The conductivity across the wires is much smaller in the 1D region than

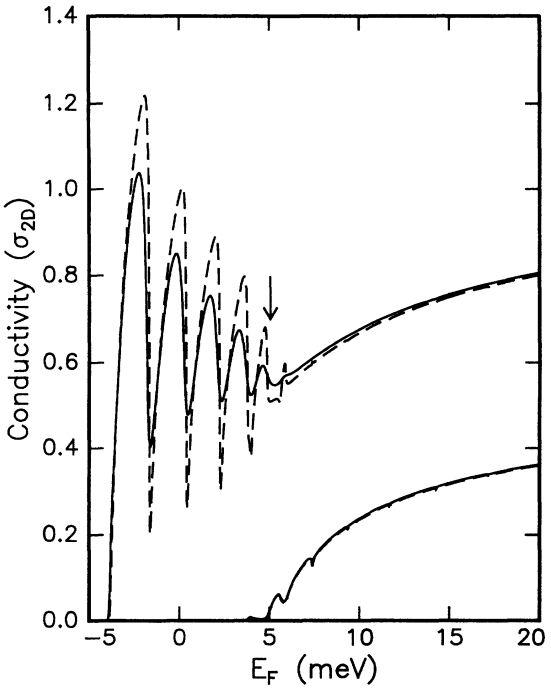

FIG. 3. Band conductivities σ^B_{xx} (upper curves) and σ^B_{yy} (lower curves) in units of the conductivity of a 2DEG, $\sigma_{2D}(E_F)$, in dependence on Fermi energy. The parameters are the same as in Fig. 1 and the scattering strengths correspond to $\mu_{2D} = 5\times10^4$ cm^2/V s (solid line) and $\mu_{2D} = 5\times10^5$ cm^2/V s (dashed line).

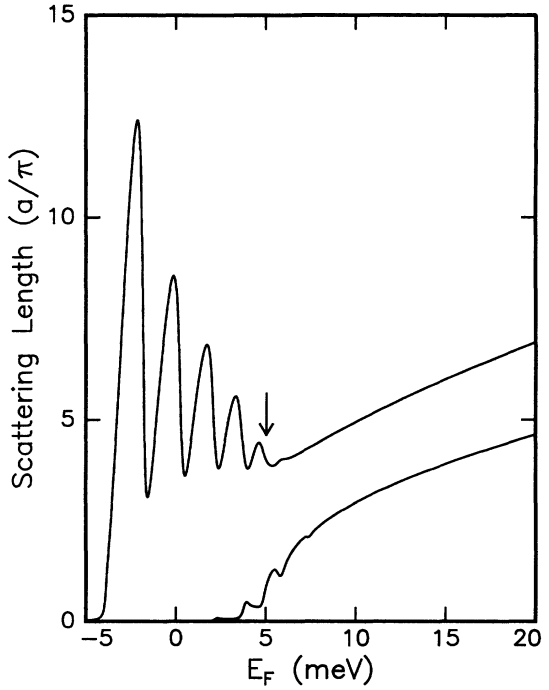

FIG. 4. Scattering lengths l_x (upper curve) and l_y (lower curve) in units of a/π in dependence on Fermi energy. The scattering strength corresponds to $\mu_{2D} = 5\times10^4$ cm^2/V s and otherwise the same parameters as in Fig. 1 have been used.

that along the wires, but it is finite due to the possibility of tunneling. Its energy dependence becomes two dimensional for $E_F > V_0$ as that of σ_{xx}, but it is smaller in amplitude due to the lower density of electrons which can move freely into this direction.

From the conductivity tensor one can obtain the tensor of diffusion coefficients with the help of the Einstein relation

$$D_{ii}(E_F) = \sigma^B_{ii}(E_F)/e^2\varrho(E_F)\,. \tag{3.2}$$

The diffusion coefficients are related to the scattering lengths $l_i(E_F)$ by

$$l_i^2(E_F) = \hbar D_{ii}(E_F)/\Gamma(E_F)\,. \tag{3.3}$$

The latter are shown in Fig. 4 in dependence on Fermi energy for a scattering strength corresponding to $\mu_{2D} = 5\times10^4$ cm^2/V s and otherwise the same parameters as in Fig. 1. The scattering length l_x along the equipotential lines is seen to be much larger than the potential period and subband effects are well resolved. This results in the pronounced oscillations of l_x in the one-dimensional region ($E_F < V_0$) where it increases almost linearly with Fermi energy followed by abrupt drops at the subband bottoms. Above the threshold it behaves as in two dimensions: $l_x \sim \sqrt{E_F}$. The scattering length l_y in direction of the potential modulation becomes very small in the 1D region as expected from the small group velocity in this direction. For $E_F > V_0$ it shows a 2D energy dependence as l_x but has a smaller absolute value as discussed for the conductivity. Close to the threshold one recognizes the influence of the finite bandwidth due to the enhanced tunneling between different potential wells.

B. Weak-localization correction to conductivity

The method to incorporate weak localization into calculations of the conductivity of low-dimensional systems is described in detail in Ref. 15 where it has been applied to a single quantum wire. Within this method a self-consistent treatment of the cooperon allows one to investigate the transition from weak to strong localization and to estimate the localization length. For a modulated 2DEG the result for the conductivity is

$$\sigma_{ii}(E_F) = \frac{e^2}{h}\sum_{n\mathbf{k}} \hbar^2 v_i^2 A^2_{n\mathbf{k}}(E_F)\,[1 + F_{n\mathbf{k}}(E_F)]^{-1} \tag{3.4}$$

with

$$F_{n\mathbf{k}}(E_F) = g^{\rm el} C(E_F) A_{n\mathbf{k}}(E_F)/\Gamma(E_F)\,. \tag{3.5}$$

In Eq. (3.5) $C(E_F)$ represents the cooperon averaged over the potential period as it has been done for the one-particle self-energy. Note that the cooperon term appears in the denominator of the relation for the conductivity as a result of the above mentioned self-consistency.

In real space, the cooperon is given by the integral

equation[15,25]

$$C(\mathbf{r},\mathbf{r}';E_F) = \delta(\mathbf{r}-\mathbf{r}') + \int d^2\mathbf{r}''\, I(\mathbf{r},\mathbf{r}'';E_F)C(\mathbf{r}'',\mathbf{r}';E_F)\,,$$
$$I(\mathbf{r},\mathbf{r}';E_F) = g^{\rm el}\, G^R(\mathbf{r},\mathbf{r}';E_F)G^A(\mathbf{r},\mathbf{r}';E_F)\,, \qquad (3.6)$$

where the $G^{R/A}(\mathbf{r},\mathbf{r}';E_F)$ denote the retarded and advanced Green functions, respectively, in self-consistent Born approximation. After averaging over the period a the approximate solution for the cooperon can be written as

$$C(E_F) \equiv C(\mathbf{r},\mathbf{r};E_F) = \sum_{m,\mathbf{q}} [1 - I_m(\mathbf{q})]^{-1}\,,$$
$$I_m(\mathbf{q}) = g^{\rm el} \sum_{n,n',\mathbf{k}} \mid a^m_{n,n'}(q_y,k_y) \mid^2 \times G^R_n(\mathbf{q}-\mathbf{k})G^A_{n'}(\mathbf{k}) \qquad (3.7)$$

with the coefficients

$$a^m_{n,n'}(q_y,k_y) = \int_a \frac{dy}{a}\, u_{n,k_y-q_y}(y)e^{2\pi i m y/a}u^*_{n',k_y}(y)\,. \qquad (3.8)$$

It reduces to the expressions derived in Ref. 15 in the limit of an isolated quantum wire if the spectrum shows no dispersion in the y direction and to the usual expressions for a 2D system for vanishing modulation potential. For $L_\Phi \gg a$ the term with $m = 0$ dominates the sum in Eq. (3.7) which results in

$$C(E_F) \approx \sum_{\mathbf{q}} \left[\Delta_\Phi + l_x^2 q_x^2 + l_y^2 q_y^2\right]^{-1} = \frac{1}{4\pi l_x l_y}\int_\tau^\infty \frac{dt}{t}\,{\rm erf}\left[\frac{\pi l_y}{a}(t/\tau)^{1/2}\right] e^{-t/\tau_\Phi} \qquad (3.9)$$

after an expansion for small $\mathbf{q}$ ($\Delta_\Phi \ll 1$). Here Δ_Φ is given by Eq. (2.6), $\tau_\Phi = \hbar/\Gamma_{\rm in}$ is the phase coherence time, l_x and l_y are the scattering lengths defined in Eq. (3.3), and t has the dimension of a time. The integration over $\mathbf{q}$ in the first line of Eq. (3.9) is restricted to the first Brillouin zone in the y direction due to $L_\Phi \gg a$. In the second line the solution for the cooperon has been rewritten slightly to introduce the total scattering time $\tau = \hbar/\Gamma$ as the necessary short-time cutoff.[24] It enters there in an isotropic manner rather than a cutoff length would do in the first line. The limiting cases of Eq. (3.9) are

$$\begin{aligned} C(E_F) &= L_\Phi/2l_x^2 a, & L^y_\Phi &\ll a \\ C(E_F) &= (1/2\pi l_x l_y)\ln(L_\Phi/l_x)\,, & L^y_\Phi &\gg a \end{aligned} \qquad (3.10)$$

where we have introduced the phase coherence length in the y direction, $L^y_\Phi = \sqrt{D_{yy}\tau_\Phi}$. An estimate for the simple model of a cosine band gives $L^y_\Phi \sim (m^*/m^*_y)L^{\rm 2D}_\Phi \sim (U_0/\Delta E)L^{\rm 2D}_\Phi$. Here $L^{\rm 2D}_\Phi$ is the phase coherence length of the 2D system, m^*_y is the band mass in the y direction, which is inversly proportional to the bandwidth U_0 and increases exponentially with the period a, and $\Delta E = \pi^2\hbar^2/2m^*a^2$.[21] For the case of open Fermi surfaces our results are in qualitative agreement with those found in Refs. 17–19 in a different context. According to Eq. (3.10) the cooperon acquires its one-dimensional form for $l_y \to 0$ and behaves as in two dimensions for $l_y \sim l_x \gg a$. This means that the 1D-2D transition in weak localization effects takes place in coupled wires when the electrons become able to tunnel between different wires without losing phase coherence, i.e., if L^y_Φ becomes *larger* than the modulation period. This has to be distinguished from the usual 1D-2D transition in an isolated wire discussed, e.g., in Ref. 13, which takes place if the phase coherence length becomes *smaller* than the wire width. The latter transition would be caused by terms with $m \neq 0$ in Eq. (3.7). Note that the transversal diffusion coefficient introduced in Ref. 13 should not be interchanged with D_{yy} because the former does not fulfill an Einstein relation due to the vanishing conductivity in the y direction for an isolated wire.

If interference effects are neglected the quantity $F_{n\mathbf{k}}(E_F)$ is zero and Eq. (3.4) reduces to the Born approximation Eq. (3.1). For weak interference effects, i.e., not too large phase coherence length, one can expand the denominator in Eq. (3.4) which yields the usual perturbational relation

$$\sigma_{ii}(E_F) = \sigma^B_{ii}(E_F) - \Delta\sigma_{ii}(E_F),$$
$$\Delta\sigma_{ii}(E_F) = \frac{e^2}{h}g^{\rm el}\frac{C(E_F)}{\Gamma(E_F)}\sum_{n\mathbf{k}}\hbar^2 v_i^2 A^3_{n\mathbf{k}}(E_F)\,. \qquad (3.11)$$

Using $A^3_{n\mathbf{k}}(E_F) \approx 3A^2_{n\mathbf{k}}(E_F)/\Gamma(E_F)$ for weak scattering this can be rewritten as

$$\Delta\sigma_{ii}(E_F) \approx 3\frac{e^2}{\pi\hbar}l_i^2(E_F)C(E_F)\,. \qquad (3.12)$$

This gives the well known expressions

$$\Delta\sigma^{\rm 1D}_{xx}(E_F) = \frac{3}{2}\frac{e^2}{\pi\hbar}\frac{L_\Phi}{a}\,,$$
$$\Delta\sigma^{\rm 2D}_{xx}(E_F) = \frac{3}{2}\frac{e^2}{\pi^2\hbar}\ln(L_\Phi/l_x) \qquad (3.13)$$

in the 1D and 2D limits, respectively. The factor 3/2 in Eqs. (3.13) arises from the full self-consistency of the calculations. The small parameter for the above expansion is[15]

$$\delta = 4g^{\rm el}C(E_F)/\Gamma^2(E_F) \approx \frac{4}{3}\frac{\Delta\sigma_{ii}(E_F)}{\sigma^B_{ii}(E_F)}\,. \qquad (3.14)$$

It has the limits $\delta_{\rm 1D} = L_\Phi/Nl_x$ and $\delta_{\rm 2D} = (4/\pi k_F l_x)\ln(L_\Phi/l_x)$ where N is the number of occupied subbands in the 1D limit and k_F is the Fermi wave vector. Since δ becomes larger with increasing phase coherence length and decreasing electron density the conductivity approaches

$$\sigma_{ii} \approx (1+\delta)^{-1}\sigma^B_{ii} \to 0\,, \qquad (3.15)$$

which describes the transition to strong localization. The correction due to interference effects is now no longer additive in the conductivity but in the *resistiv-*

ity. The application of Eq. (3.11) would result in a negative conductivity in that case. The relative correction $\Delta\sigma_{ii}(E_F)/\sigma_{ii}^B(E_F)$ is shown in Fig. 5 in dependence on Fermi energy for two different ratios of inelastic to total scattering strength. They correspond to phase coherence lengths of about 1 μm (lower curve) and 3 μm (upper curve). One recognizes a steplike increase with decreasing Fermi energy in the 1D regime due to the depopulation of 1D subbands. For low electron densities and weak inelastic scattering interference effects contribute considerably to the total conductivity and the perturbative result Eq. (3.11) is not applicable. If the Fermi energy becomes larger than the potential amplitude the conductivity correction is much smaller and only weakly dependent on energy as expected for a 2DEG. The minima close to the threshold are due to the finite widths of the minibands leading to 2D behavior of weak localization. They become more pronounced for larger L_Φ when 1D behavior is preserved to larger Fermi energies.

The expansion parameter δ can be used to estimate the localization length $l_{\rm loc}$ in our system from the assumption that the interference effects begin to dominate the conductivity if L_Φ becomes larger than $l_{\rm loc}$,

$$\delta(L_\Phi = l_{\rm loc}) = 1\,. \tag{3.16}$$

The localization length obtained from Eq. (3.16) fulfills the correct relations in the limiting cases

$$\begin{aligned} l_{\rm loc}^{\rm 1D} &= N l_x\,, \\ l_{\rm loc}^{\rm 2D} &= l_x \exp(\pi k_F l_x/4)\,. \end{aligned} \tag{3.17}$$

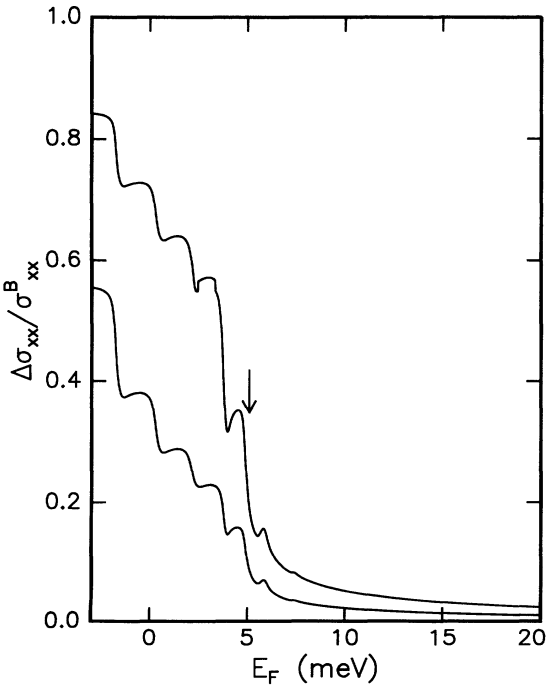

FIG. 5. Relative correction $\Delta\sigma_{ii}(E_F)/\sigma_{ii}^B(E_F)$ in dependence on Fermi energy for $\Delta_\Phi = 0.1$ (lower curve) and $\Delta_\Phi = 0.01$ (upper curve). The other parameters are the same as in Fig. 4.

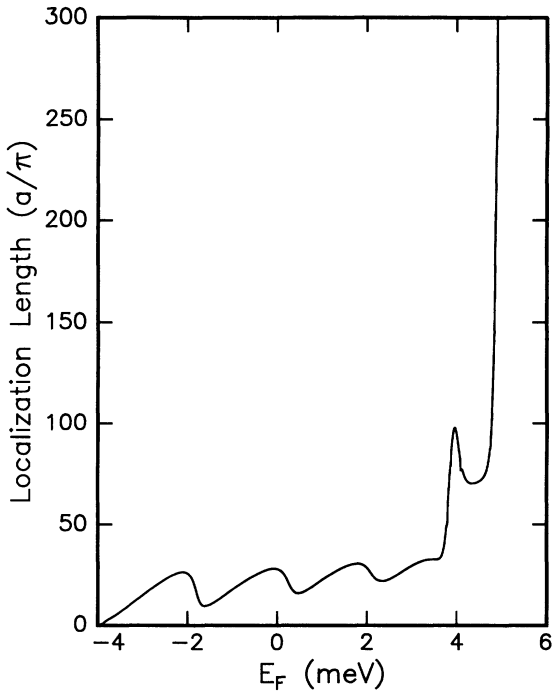

FIG. 6. Localization length $l_{\rm loc}$ in units of a/π in dependence on Fermi energy. The parameters are the same as those of Fig. 4.

In Fig. 6, we have depicted the dependence of $l_{\rm loc}$ on Fermi energy. By inspection, we find three distinct regimes. For Fermi energies below 3.5 meV the localization length behaves as in one dimension, i.e., it fulfills approximately the first relation in Eq. (3.17). For $E_F \sim 4$ meV the result clearly deviates from the 1D behavior. It is just in this energy range that the highest miniband below the potential maximum which already shows weak dispersion in the y direction is populated. The corresponding scattering length l_y becomes comparable with the period a. Hence $L_\Phi^y > a$, and the electrons are allowed to tunnel coherently between neighboring wires. Close to the potential maximum the system reaches the third regime: $l_{\rm loc}$ rises exponentially with Fermi energy as characteristic for a two-dimensional system. It is interesting to note that the different localization regimes are well resolved even for the relatively low mobility $\mu_{\rm 2D}$ of 5×10^4 cm^2/Vs due to the strongly differing energy dependences of the localization length in one and two dimensions, respectively.

IV. CONCLUSIONS

We have studied the conductivity of a 2DEG subject to a periodic potential of cosine shape in one direction with emphasis on the properties of interference effects in dependence on electron density. With decreasing density the system develops from a weakly modulated 2DEG to an array of quantum wires. A transition from 2D to 1D behavior of the weak localization correction to conduc-

tivity takes place if coherent tunneling of the electrons between adjacent wires is no longer possible. This occurs when the transversal phase coherence length related to the diffusion coefficient in the direction perpendicular to the wires becomes smaller than the potential period. We have presented numerical results for the conductivity in dependence on Fermi energy showing the gradual change from the 2D to the 1D limit and have analyzed the region in between where the Fermi energy is comparable to the potential amplitude. In the 1D limit the system rapidly undergoes a transition from weak to strong localization with decreasing electron density and increasing phase coherence length. It has been incorporated into our calculations via a self-consistent treatment of the interference effects. This allows us to estimate the localization length of the system which changes from an exponential to a linear dependence on scattering length. The conductivity correction due to interference effects becomes additive in the resistance in this case.

ACKNOWLEDGMENTS

M.S. acknowledges financial support by the DFG (Sonderforschungsbereich 348 – Teilprojekt YD). P.E.S. is greatful to the GOS e.V., Berlin.

[1] D. Weiss, K. v. Klitzing, K. Ploog, and G. Weimann, Europhys. Lett. **8**, 179 (1989).
[2] R. W. Winkler, J. P. Kotthaus, and K. Ploog, Phys. Rev. Lett. **62**, 1177 (1989).
[3] R. R. Gerhardts, D. Weiss, and K. v. Klitzing, Phys. Rev. Lett. **62**, 1173 (1989).
[4] C. W. J. Beenakker, Phys. Rev. Lett. **62**, 2020 (1989).
[5] K. Ismail, W. Chu, D. A. Antoniadis, and H. I. Smith, Appl. Phys. Lett. **52**, 1071 (1988).
[6] J. Alsmeier, Ch. Sikorsky, and U. Merkt, Phys. Rev. B **37**, 4314 (1988).
[7] F. Brinkop, W. Hansen, J. P. Kotthaus, and K. Ploog, Phys. Rev. B **37**, 6547 (1988).
[8] P. H. Beton, E. S. Alves, P. C. Main, L. Eaves, M. W. Dellow, M. Henini, O. H. Hughes, S. P. Beaumont, and C. D. W. Wilkinson, Phys. Rev. B **42**, 9229 (1990).
[9] G. Berthold, J. Smoliner, W. Demmerle, F. Hirler, E. Gornik, W. Ettmüller, G. Böhm, and G. Weimann, Semicond. Sci. Technol. **6**, 709 (1991).
[10] H. L. Störmer, L. N. Pfeiffer, K. W. West, and K. W. Baldwin, in *Nanostructures and Mesoscopic Systems*, edited by W. P. Kirk and M. A. Reed (Academic, Boston, 1992), p. 51.
[11] M. J. Kelly, J. Phys. C **18**, 6341 (1985).
[12] P. F. Bagwell and T. P. Orlando, Phys. Rev. B **40**, 3735 (1989).
[13] M. J. Kearney and P. N. Butcher, J. Phys. C **21**, 2539 (1988).
[14] M. Suhrke, S. Wilke, and R. Keiper, Solid State Commun. **76**, 551 (1990).
[15] M. Suhrke and S. Wilke, Phys. Rev. B **46**, 2400 (1992).
[16] P. Wölfle and R. N. Bhatt, Phys. Rev. B **30**, 3542 (1984).
[17] V. N. Prigodin and Yu. A. Firsov, Pis'ma Zh. Eksp. Teor. Fiz. **38**, 241 (1983) [JETP Lett. **38**, 284 (1983)]; Yu. A. Firsov and V. N. Prigodin, Solid State Commun. **56**, 1069 (1985).
[18] E. P. Nakhmedov, V. N. Prigodin, and Yu. A. Firsov, Pis'ma Zh. Eksp. Teor. Fiz. **43**, 575 (1986) [JETP Lett. **43**, 743 (1986)] .
[19] N. Dupuis and G. Montambaux, Phys. Rev. Lett. **68**, 357 (1992); Phys. Rev. B **46**, 9603 (1992).
[20] W. Szott, C. Jendrzejek, and W. P. Kirk, Superlatt. Microstruct. **11**, 199 (1992).
[21] J. C. Slater, Phys. Rev. **87**, 807 (1952).
[22] D. Weiss, C. Zhang, R. R. Gerhardts, K. v. Klitzing, and G. Weimann, Phys. Rev. B **39**, 13 020 (1989).
[23] B. L. Altshuler, A.G. Aronov, D. E. Khmelnitskii, and A. I. Larkin, in *Quantum Theory of Solids*, edited by I. M. Lifshits (Mir Publishers, Moscow, 1982), p. 130.
[24] G. Bergmann, Phys. Rep. **107**, 1 (1984).
[25] A. D. Stone, in *Physics of Nanostructures*, edited by J. H. Davies and A. R. Long (SUSSP Publications and IOP Publishing, Bristol, 1992), p. 65.